

NUMERICAL CALCULATIONS OF THE MOBY DICK EXPERIMENT BY MEANS OF UNSTEADY RELAXATION MODEL

MARIUSZ BANASZKIEWICZ

DARIUSZ KARDAŚ

Institute of Fluid-Flow Machinery Polish Academy of Sciences, Gdańsk
e-mail: tjan@imppan.imr.pg.gda.pl

The paper presents numerical calculations of the Moby Dick experiment by means of the nonequilibrium relaxation model. Calculations are made using a computer code for solving non-steady flow problems. An interesting problem discussed in the paper is an appropriate choice of correlations for the relaxation time as well as a suitable value of the friction factor which have an effect on the process of vapour production in the model. The obtained numerical results appear to be in a reasonable agreement with the experimental data. This agreement speaks in favour of the homogeneous relaxation model as a useful tool for describing critical flows of water and vapour.

Key words: two-phase flow, flashing, pseudo-criticality, thermal nonequilibrium

1. Introduction

Single-component two-phase flows are of particular interest for their unique properties, different from those revealed by other flows common in industry and nature. Above all, it refers to the flows of water and its vapour at near-critical velocities when the processes of interfacial interaction begin to play a dominant role. These processes are met neither in single-phase flows nor in multi-component flows. They give rise to creation of the so-called pseudo-critical flow which occurs before the full choking of the channel. The pseudo-critical flow is distinct by virtue of small changes in the mass flow rate during considerable backpressure drops – a phenomenon not observed in other kinds of flows.

Also, the values of critical velocity in two-phase flows under given stagnation conditions can be astounding. The critical velocity turns out to be much lower than the speed of sound in pure water or vapour. It varies with the volumetric fraction of phases in the two-phase mixture. The local and also the critical velocity are determined by the rate of creation and growth of the new phase. The above phenomena under some conditions act towards equating these velocities driving the flow to the limit of choking.

Numerous experiments carried out heretofore prove the existence of thermodynamic nonequilibrium between the coexisting phases. It manifests itself by a temperature difference between the water and vapour, where the temperature of the vapour is the saturation temperature for a given pressure and the water remains in a metastable state. It means that the phase transition is not equilibrium one and is characterised by some delay measure of which is superheating of the water phase.

Besides the temperature difference between both phases, usually an interfacial slip is observed, that is the liquid and the vapour have different velocities. This adds a mechanical nonequilibrium to the two-phase system. This nonequilibrium appears to be the strongest in places of creation of the new phase. The fact that critical two-phase flows are nonequilibrium flows should be taken into account in their modelling. The lack of local thermal equilibrium between the phases is also a result of inertia of the governing processes. The mass, momentum and energy exchange in real phenomena does not occur instantaneously but takes place at a limited rate, characteristic for a given process. This should also be accounted for in the flow model.

In this paper, a homogeneous relaxation model is applied to numerical calculations of two-phase flows of water and vapour with thermodynamic nonequilibrium. The calculations are made using a computer code for solving non-steady problems and converge to a steady state. The obtained results are compared with the Moby Dick experiments well known in the literature (cf Reocreux (1974)).

2. Description of the experiment

The Moby Dick experiment was performed at the Centre d'Etudes Nucleaires in Grenoble (France) in early seventies. Carried out with an extraordinary care and well documented, has served as a basis for understanding critical two-phase single-component flows ever since its publication. This experiment has been performed on a very complicated installation, where a working medium

was the hot water. The water was decompressed in the diffuser, what caused its rapid evaporation and creation of a two-phase bubble mixture. The measurements were made in a vertical channel consisting of a straight pipe of the inside diameter 20 mm followed by a conical expander of the length 327 mm diverging at 7°. The exit from the divergent cone was connected to the condenser by considerably long piping of the inside diameter 60 mm. A scheme of the channel and its dimensions are shown in Fig.1.

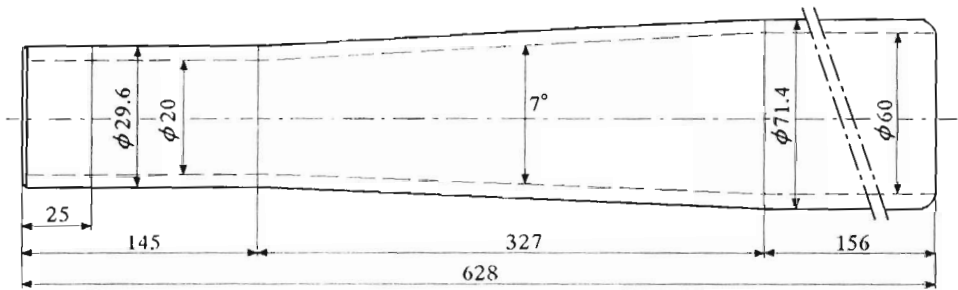


Fig. 1. The channel used in the Moby Dick experiments (cf Reocreux (1974))

The shape and dimensions of the nozzle were selected so as to assure one-dimensional flow regime and eliminate the effects of rapidly changing shape. Thermodynamic parameters (pressure and temperature) of hot water flowing into the test section were kept constant during the measurements. However, the backpressure in the condenser varied, giving an impact on the mass flow rate at the inlet. The void fraction was measured in the test section by means of a γ -ray absorption method. The pressure was also measured there. Besides, the temperature and mass flow rate at the inlet as well as the temperature in the condenser were measured. Typical pressure and void fraction profiles for a single series of measurements are shown in Fig.2 and Fig.3 (cf Reocreux (1974)). Values of the flow parameters are given in Table 1.

Table 1

Run	T_{in} [°C]	P_{in} [bar]	P_{out} [bar]	G [kg/(m ² s)]
423	121.9	1.918	1.359	4383
424	121.8	1.914	1.430	4357
425	121.7	1.915	1.491	4355
426	121.8	1.939	1.531	4360
427	121.8	1.939	1.619	4345
428	121.8	1.912	1.712	4331

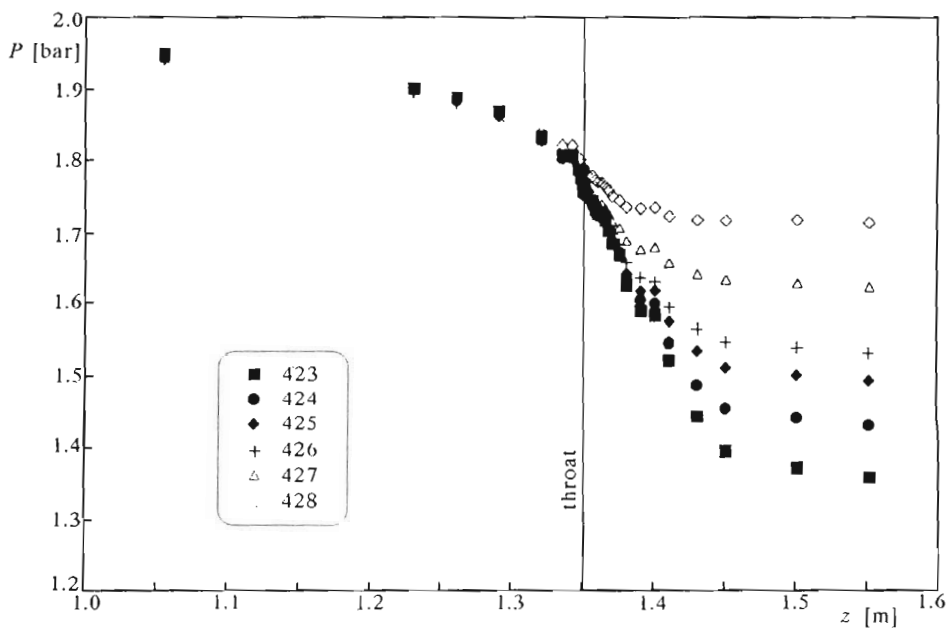


Fig. 2. Typical pressure profiles for runs 423 ÷ 428 after Reocreux (1974)

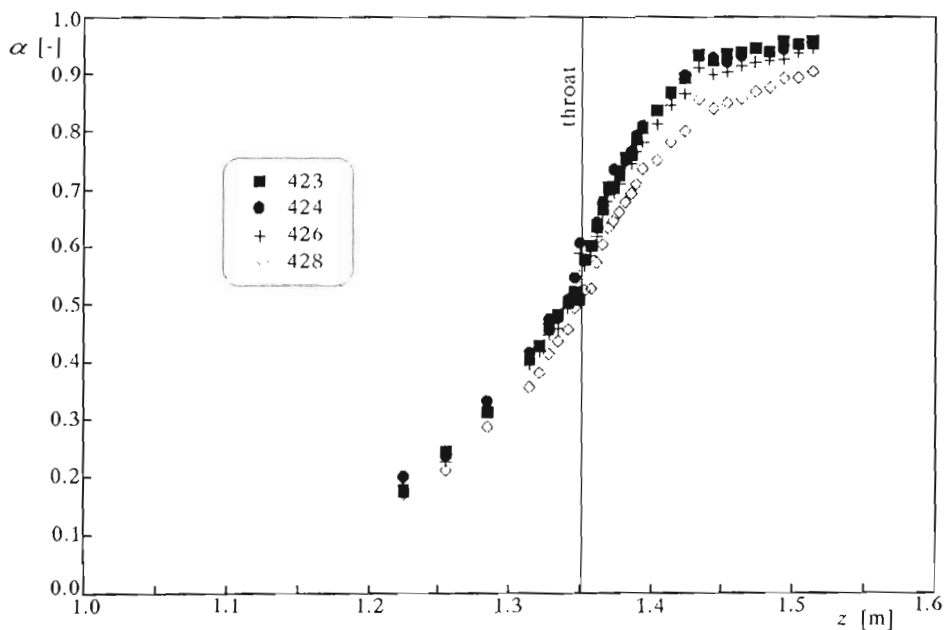


Fig. 3. Typical void fraction profiles for runs 423 ÷ 428 after Reocreux (1974)

Reocreux and his collaborators interpreted these flows as choked at the throat. They admitted that the flow was subcritical before the throat, supercritical behind it and overrunning the limit of sound took place close to the throat. They considered the throat as a place of choking because of its minimum cross-section area, therefore the velocity of the choked flow should reach the speed of sound there. Choking of the flow was indicated by the fact that reducing the backpressure in the condenser did not increase the flow rate at the inlet.

The only surprising thing was the lack of a shock wave which always appears in the compressible flow within the supercritical section of the nozzle.

An explanation of this fact can be found in Bilicki et al. (1990), who gave a reinterpretation of the experimental results. An additional circumstance for this interpretation, different than that of Reocreux, was small superheating of the liquid ($2 \div 3^\circ\text{C}$) observed during the tests due to some delay in evaporation. For runs 400 \div 402 the liquid flowed 0.4 m under metastable conditions and the vapour bubbles were observed close to the throat. As a result of their investigations, Bilicki et al. (1990) postulated that due to the thermodynamic nonequilibrium, the flow in the nozzle is subcritical and is choked at the inlet to the condenser. The support for this hypothesis was given on the basis of homogeneous relaxation model (cf Bilicki and Kestin (1990)) that assumes the existence of thermodynamic nonequilibrium between the liquid and the vapour and represents scribes nonequilibrium generation of the vapour by means of a relaxation-type evolution equation. Unlike in the equilibrium model which assumes equilibrium production of the vapour, their calculations carried out with the help of the nonequilibrium model made it possible to interpret correctly the results of void fraction measurements. The reinterpretation of the Moby Dick experiment is as follows:

- The throat of the nozzle is not a place of critical transition (the relaxation model does not predict a saddle point there)
- Lack of a shock wave is caused by the subcritical conditions existing in the entire nozzle
- The flow velocity in the entire nozzle is lower than the frozen speed of sound
- The flow is choked but as a result of nonequilibrium production of the vapour the critical cross-section is close to the condenser.

3. Nonequilibrium relaxation model

A basis for the nonequilibrium relaxation model are the conservation equations written for mass, momentum and energy of the mixture and an evolution equation for the nonequilibrium dryness fraction. In principle, it is a partly nonequilibrium model in regard of thermodynamics, because it assumes that the vapour remains under saturation conditions and the liquid is in a metastable state. Moreover, it assumes that the velocity difference between the phases is negligible and their pressures are equal.

The model consists then of four equations written in the so called quasi-one-dimensional approximation:

— mass conservation for the mixture

$$\frac{\partial \rho}{\partial t} + \frac{1}{A} \frac{\partial A \rho w}{\partial z} = 0 \quad (3.1)$$

— momentum conservation for the mixture

$$\frac{\partial w}{\partial t} + \frac{1}{2} \frac{\partial w^2}{\partial z} + \frac{1}{\rho} \frac{\partial p}{\partial z} = -\frac{\tau_w}{\rho} + g \quad (3.2)$$

— internal energy conservation for the mixture

$$\frac{\partial \rho u}{\partial t} + \frac{1}{A} \frac{\partial \rho w u A}{\partial z} + \frac{P}{A} \frac{\partial w A}{\partial z} = \tau_w w \quad (3.3)$$

— vapour production

$$\frac{\partial x}{\partial t} + w \frac{\partial x}{\partial z} = \frac{\Gamma_v}{\rho} \quad (3.4)$$

Left-hand sides of these equations contain independent variables which describe the state of the two-phase mixture and constitute the state vector consisting of the velocity w , the pressure p , multiple of the density and the internal energy ρu , and the nonequilibrium dryness fraction x . On the right-hand side we have source terms and external interactions forces. They are as follows: the friction force τ_w , the gravity force g and the volumetric vapour source Γ_v .

The equilibrium dryness fraction, which would exist in an equilibrium mixture of dry saturated vapour and boiling water at the same pressure and enthalpy, will be denoted by \bar{x} . It can be calculated from the caloric or thermal equation of state written for the mixture being in the thermodynamic equilibrium

$$\bar{x} = \frac{h - h_l}{h_v - h_l} \quad (3.5)$$

or, equivalently

$$\bar{x} = \frac{v - v_l}{v_v - v_l} \quad (3.6)$$

where the specific enthalpies and the specific volumes are taken from the vapour-pressure line and are functions of the pressure only.

A complete description of the flow requires closures in the form of constitutive equations for the fluxes which appear in the conservation equations. In our case there are four equations:

— thermal equation of state

$$v = xv_v + (1 - x)v_l \quad (3.7)$$

where the specific volume of the vapour is taken from the vapour-pressure line $v_v = v_v(p)$, and the specific volume of the liquid is calculated in the metastable region $v_l = v_l(p, T_l)$;

— caloric equation of state

$$h = xh_v + (1 - x)h_l \quad (3.8)$$

where the specific enthalpy of the vapour is taken from the vapour-pressure line of saturation $h_v = h_v(p)$, and the specific enthalpy of the liquid is calculated in the metastable region $h_l = h_l(p, T_l)$. These functions have been calculated on the basis of thermodynamic functions for water and vapour in the metastable region (cf Kardaś and Bilicki (1991));

— wall shear stress equation

$$\tau = \frac{C}{2A} f \rho w^2 \quad (3.9)$$

— rate equation

$$\frac{\Gamma_v}{\rho} = -\frac{x - \bar{x}}{\theta} \quad (3.10)$$

4. Closure equations

4.1. Friction force

The friction pressure drop in a single-phase part of the flow may be calculated from the classical formula

$$\tau = \frac{C'}{2A} f \rho w |w| \quad (4.1)$$

where

- C – channel perimeter
- A – cross-section area
- f – friction factor dependent on the Reynolds number.

This formula describes the friction force in a single-phase flow. Due to the appearance of vapour bubbles at the wall of the channel, it can be expected that the flow resistance will increase. So will the pressure drop. In this case, the correction factor dependent on the amount of the vapour in the mixture has to be introduced into Eq (4.1), what can be written as follows

$$\tau_w = \Phi^2 \tau \quad (4.2)$$

where

- τ_w – frictional pressure drop of the two-phase mixture
- τ – frictional pressure drop for the liquid flow
- Φ – two-phase factor.

The simplest two-phase multiplier Φ is evaluated from the Lockhart-Martinelli correlation modified by Richardson (1958)

$$\Phi^2 = (1 - \alpha)^{-1.75} \quad (4.3)$$

4.2. Relaxation equation

The rate of production of the vapour phase in the nonequilibrium relaxation model is described by the evolution equation (cf Bilicki and Kestin (1990))

$$\frac{\partial x}{\partial t} + w \frac{\partial x}{\partial z} = - \frac{x - \bar{x}}{\theta} \quad (4.4)$$

This equation expresses the inertia of mass exchange and describes some delay caused by a finite rate at which this process takes place. If the rate was infinite then under some flow conditions the equilibrium would be reached immediately, without any delay. The difference between the equilibrium and nonequilibrium dryness fraction is a measure of departure from the equilibrium state and constitutes the drag force driving the system to this state. The bigger this difference, the more intensive evaporation. When the dryness fraction reaches its equilibrium value, the mass exchange vanishes and the vapour production stops. The relaxation time denoted here by θ is the time during which the system reaches its equilibrium state.

This simple relaxation equation, being only a linear approximation of the function L_v , has turned out to be efficient in describing very complicated processes of generation of the vapour phase. It describes the creation of new vapour bubbles of some critical radius and growth of the bubbles created earlier. This rate equation contains both homogeneous and heterogeneous nucleation, which depends not only on the flow parameters but also on the state of the fluid and the state of walls. It has been known for years and was used by Mandelstam and Leontovich (1937), however Bauer et al. (1976) were among the first to have made use of it in the context of two-phase flow (in 1976).

Serious difficulties are encountered while trying to evaluate the relaxation time in Eq (4.4). For this reason an empirical correlations are built on the basis of experimental data to enable the numerical calculations. However, due to their empirical nature, the scope of their application is confined to the conditions appropriate for these experiments. Two correlations were found on the basis of the Moby Dick experiment. One of them was formulated by Bauer et al. (1976) and it provides a relation between the local value of the relaxation time and the parameters describing the thermodynamic state of the mixture (pressure p and void fraction α) as well as the dynamic state of the flow (velocity w). The formula was given as

$$\theta = 660p^{-0.505}w^{-1.89}\alpha^{-0.954} \tag{4.5}$$

where the units of pressure and velocity are [Pa] and [m/s], respectively.

The second correlation was given by Downar-Zapolski et al. (1996). Using the least square method he approximated the experimental data and obtained the following formula

$$\theta = \theta_0\alpha^{-0.54}\varphi^{-1.76} \tag{4.6}$$

where $\theta_0 = 3.84 \cdot 10^{-7}$ has the dimension of time in seconds and

α - void fraction

φ - nondimensional pressure difference calculated as follows

$$\varphi = \frac{p_s(T_{in}) - p}{p_c - p_s(T_{in})} \tag{4.7}$$

where

p - actual pressure of the mixture

$p_s(T_{in})$ - saturation pressure corresponding to the inlet temperature

p_c - critical pressure, $p_c = 218.2$ bar.

5. Difference scheme

Unsteady two-phase flows can be computed by means of finite-volume schemes on grids with staggered nodes. The mass and energy equations are differenced over the same nodes, whereas the momentum equation is differenced over displaced nodes. This forms a staggered spatial difference scheme used by many other investigators for solving multi-phase problems. The index j refers to the scalar variables like: pressure p , density ρ , internal energy u and dryness fraction x . The velocity vector \mathbf{w} is calculated on the boundaries of the cells and the related index is the odd multiple of $1/2$.

The method used in this paper is a method of balancing the mass, momentum and energy within the mesh cells, see Kardaś (1994). To ensure stability of the solution, the balance equations are written in the conservative form with the state vector given as $\sigma = [p, \mathbf{w}, \rho u, x]$. The difference equations are supplemented with an additional relationship which adds stability to the scheme

$$f_{j+1/2} = \frac{1}{2} \left(f_j + f_{j+1} + \frac{|w_{j+1/2}|}{w_{j+1/2}} (f_j - f_{j+1}) \right) \quad (5.1)$$

While building the numerical scheme, we were driven by the principle of linearity of the scheme with respect to the variables at time step $n + 1$. The numerical scheme obtained in this way is semi-explicit with no iteration process required.

6. Results

The numerical scheme described above was employed to deal with the system of partial differential equations describing the flow under consideration. An unsteady problem with initial-boundary conditions was solved and the final results of our calculations are steady-state profiles of the flow parameters. The calculations were carried out until a constant value of the mass flow rate was reached. It made us sure that the flow of the two-phase mixture attained a steady-state velocity and density – an indication of the end of vapour production. In every case stable conditions were reached after some 1.5 s, bearing in mind that the required pressure drop at the outlet boundary, taken from the experiment, was obtained after 0.2 s. Initially, the pressure in the entire channel was equal, the velocity and dryness fraction were assumed zero. Then the pressure at the outlet boundary was decreased to the required value. At

the same time the inlet pressure was kept constant and equal to the initial value. The initial pressure was set according to the value of pressure at the inlet recorded in the experiment. The obtained pressure profiles along the channel were compared with experimental results.

The calculations were made out for runs 400, 401 and 402 in which the onset of evaporation was located close to the throat. A constant value of the friction factor $f = 0.008$ was assumed. This value is in common use for two-phase flow calculations. In order to estimate the relaxation time the correlation (4.6) put forward by Zapolski was used (cf Downar-Zapolski et al. (1996)). It has turned out that for each run, much lower mass flow rates are obtained, compared to the experiment. Additionally, they are substantially different for different runs although they were almost equal in the experiment. Also Bauer's correlation (4.5) failed to yield accurate results. On the one hand, it gives better mass flow rates for $f = 0.008$. On the other hand, the profiles of pressure and void fraction do not agree with experiment at all. Fig.4 and Fig.5 show a comparison between the calculated and experimental results. It is clearly seen that not only the mass flow rate at the inlet but also the pressure and void fraction profiles are far from the experimental values.

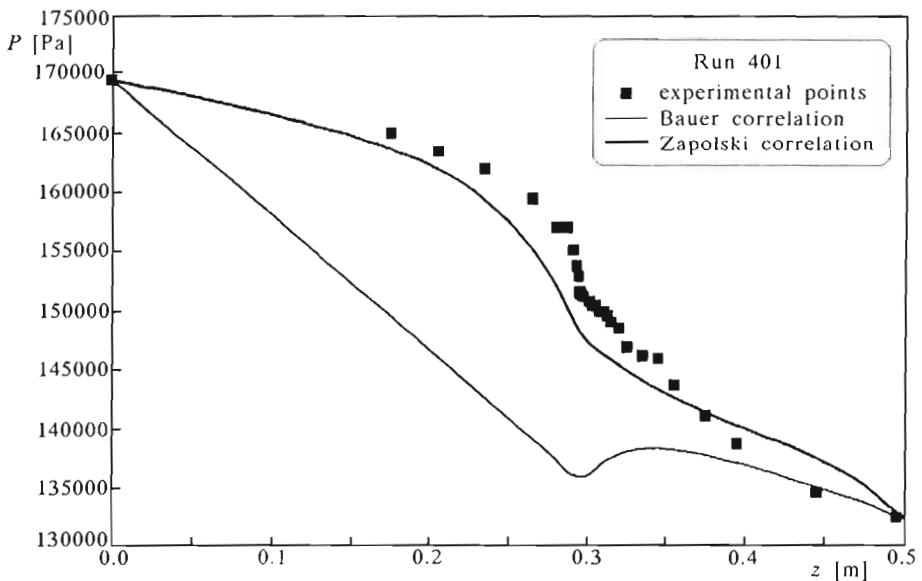


Fig. 4. Experimental pressure profile for run 401 ($G_{exp} = 6465 \text{ kg/m}^2\text{s}$) and theoretical profiles calculated with Zapolski's correlation ($G_{calc} = 2757 \text{ kg/m}^2\text{s}$) and Bauer's correlation ($G_{calc} = 4897 \text{ kg/m}^2\text{s}$) for friction factor $f = 0.008$

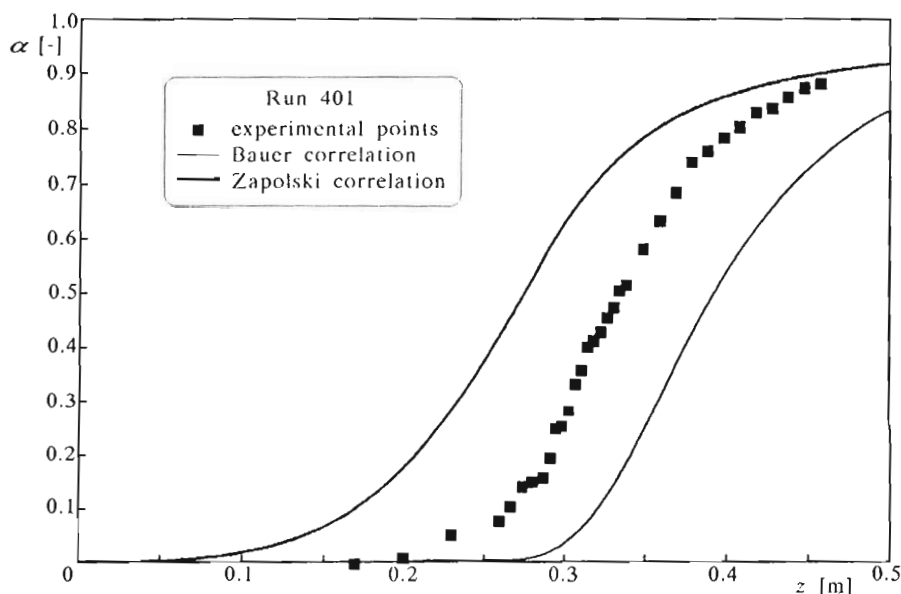


Fig. 5. Experimental void fraction profile for run 401 ($G_{exp} = 6465 \text{ kg/m}^2\text{s}$) and theoretical profiles calculated with Zapolski's correlation ($G_{calc} = 2757 \text{ kg/m}^2\text{s}$) and Bauer's correlation ($G_{calc} = 4897 \text{ kg/m}^2\text{s}$) for friction factor $f = 0.008$

An attempt to apply the correlations of Chen (1979) and Woods, see Richardson (1958) to estimation of the friction factor was also made. These correlations predict similar values $f = 0.008$ and the mass flow rate, pressure and void fraction profiles as earlier. In order to achieve a good agreement with the experiment, it is necessary to select an appropriate constant friction factor, different for every run. Examples of such calculations are shown in Fig.6 ÷ Fig.11, where the throat is marked by a vertical line. These figures show not only qualitative but also quantitative agreement of the numerical calculations with the experimental data. A very good agreement as far as the void fraction profiles attests that the relaxation equation describes well the process of nonequilibrium production of the vapour and that Zapolski's correlation was worked out correctly.

Pressure profiles in the section of the channel of constant area where the flow is still single-phase almost ideally coincide with the experimental points. This suggests also that the friction factor has been appropriately selected. The biggest differences are observed near the throat, where the numerically calculated pressure is always lower than the experimental one. It is probably

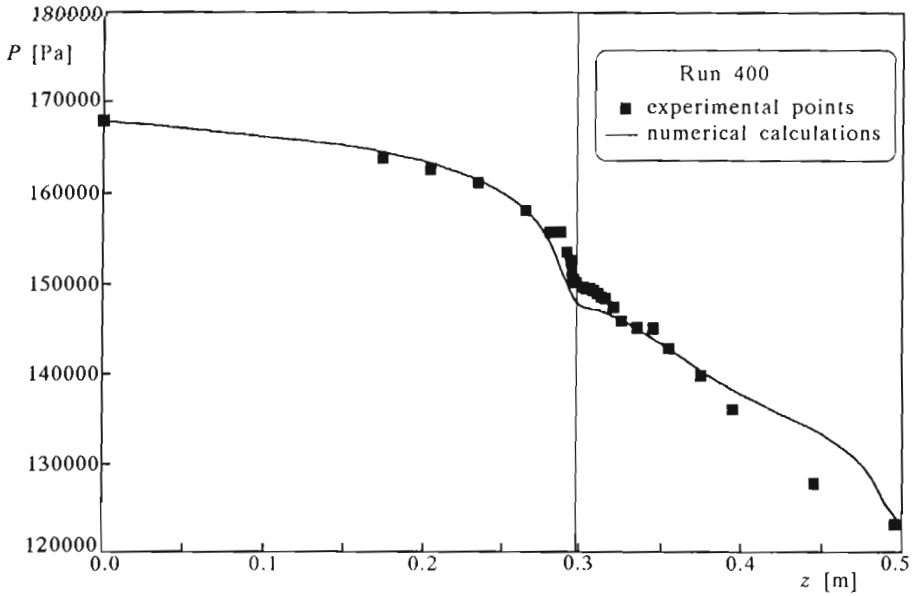


Fig. 6. Theoretical and experimental pressure profiles for run 400. Zapolski's correlation, $G_{exp} = 6526 \text{ kg/m}^2\text{s}$, $G_{calc} = 6529 \text{ kg/m}^2\text{s}$, $f = 0.00015$

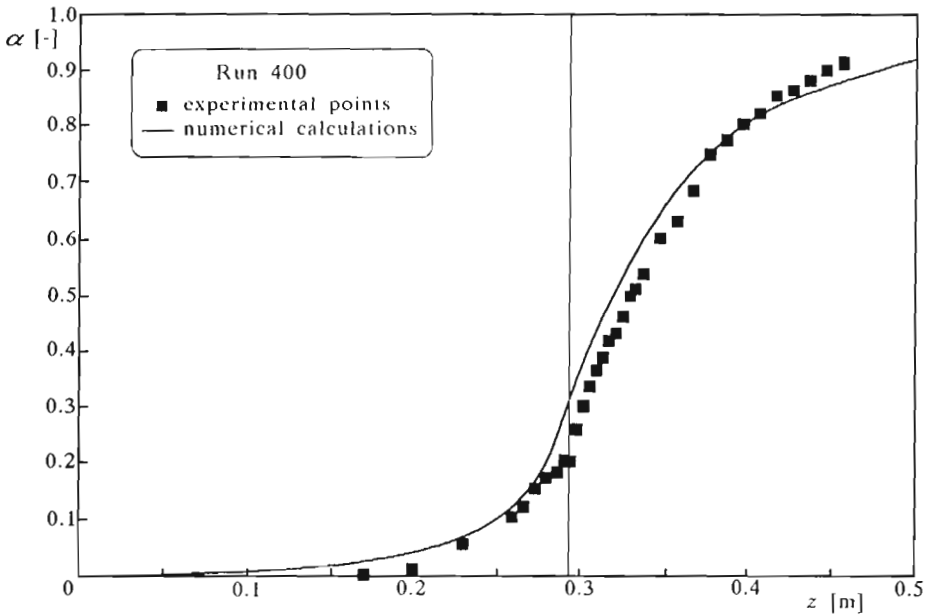


Fig. 7. Theoretical and experimental void fraction profiles for run 400. Zapolski's correlation, $G_{exp} = 6526 \text{ kg/m}^2\text{s}$, $G_{calc} = 6529 \text{ kg/m}^2\text{s}$, $f = 0.00015$

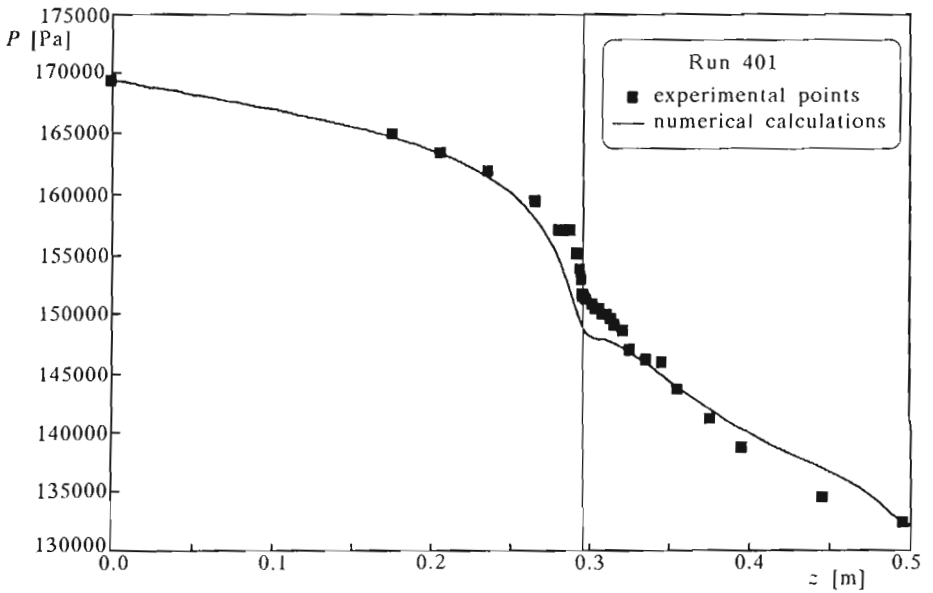


Fig. 8. Theoretical and experimental pressure profiles for run 401. Zapolski's correlation, $G_{exp} = 6465 \text{ kg/m}^2\text{s}$, $G_{calc} = 6510 \text{ kg/m}^2\text{s}$, $f = 0.0005$

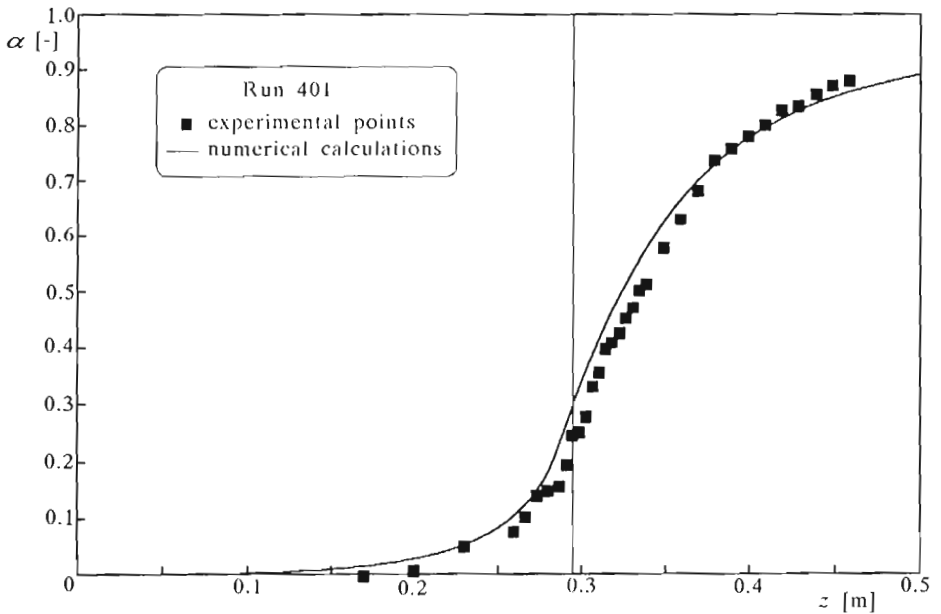


Fig. 9. Theoretical and experimental void fraction profiles for run 401. Zapolski's correlation, $G_{exp} = 6465 \text{ kg/m}^2\text{s}$, $G_{calc} = 6510 \text{ kg/m}^2\text{s}$, $f = 0.0005$

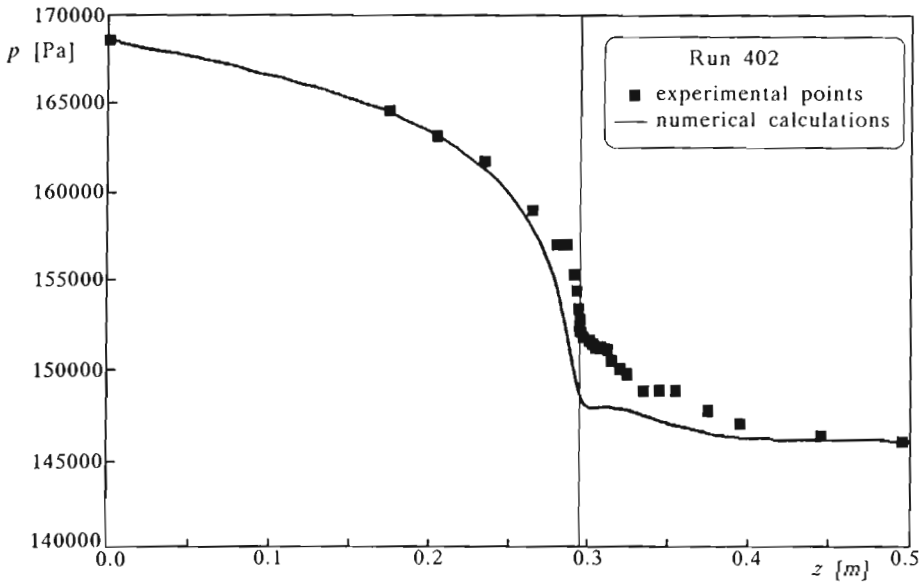


Fig. 10. Theoretical and experimental pressure profiles for run 402. Zapolski's correlation, $G_{exp} = 6496 \text{ kg/m}^2\text{s}$, $G_{calc} = 6429 \text{ kg/m}^2\text{s}$, $f = 0.00024$

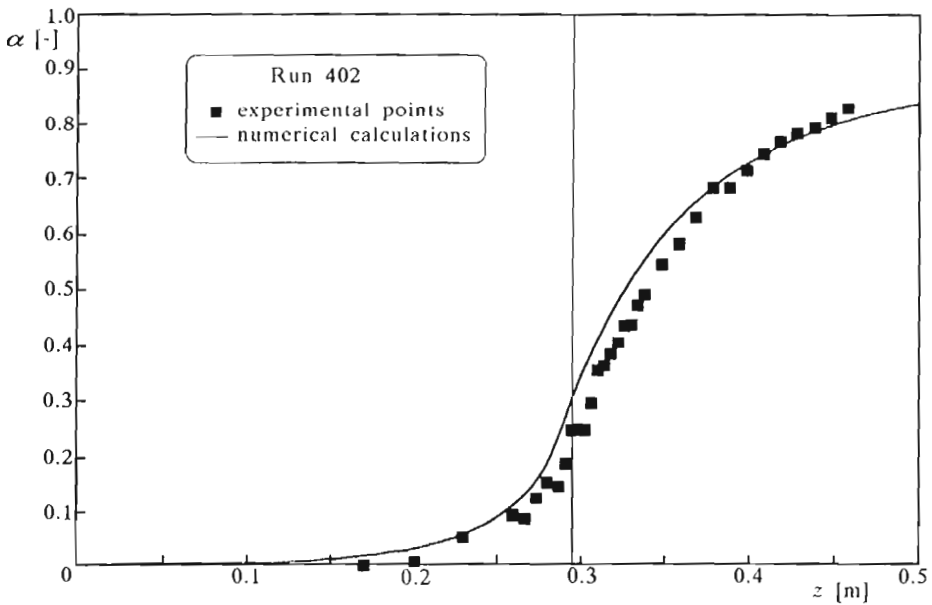


Fig. 11. Theoretical and experimental void fraction profiles for run 402. Zapolski's correlation, $G_{exp} = 6496 \text{ kg/m}^2\text{s}$, $G_{calc} = 6429 \text{ kg/m}^2\text{s}$, $f = 0.00024$

caused by vapour overproduction leading to an excessive amount of the vapour in the throat.

Moreover, the throat is a place of rapid change of the cross-section area and the largest influence of two-dimensional effects can be expected there. Understandably, the best agreement is observed at the inlet and at the outlet as a result of appropriately imposed boundary conditions taken from measurements.

Unexplained are the differences in values of the friction factor. The numerically selected friction factors were found to change with every run and be different from values given in the literature. All tested correlations predicted the minimum value of friction factor as $f = 0.008$. However, as shown in Fig.4, this value is too large for unsteady calculations and pressure drops are substantially larger than those reported by Reocreux. As a result, strong choking of the flow is obtained and the discrepancies in the mass flow rate reach $25 \div 55\%$, according to the used correlation for the relaxation time. The numerically obtained values of the friction factor are substantially lower. A constant and very small friction factor gives better results than that dependent on the flow velocity, although the latter being widely recognised in the literature. Similar results were obtained by the authors of TRAC (cf Saha et al. (1982)), where friction factors also turned out to be too large. It ensued increased flow resistance and decreased mass flow rates at the inlet.

Such substantial differences may be caused by different character of the numerical experiment solving unsteady flow problems, opposed to the surely steady-state nature of real experiments. In order to explain this problem, time-evolution of basic flow parameters is drawn in Fig.12 \div Fig.14. They are the pressure and void fraction at the throat and the mass flow rate at the inlet. The pressure and void fraction curves, being calculated with the help of Zapolski's correlation, have clear extrema observed at the same instant, 0.25s after the calculations began. The pressure drop at the outlet boundary is obtained after 0.2s, so these times are near equal. The maximum pressure agrees with the minimum void fraction, what can be explained by the fact that low pressures resulting in small relaxation times give rise to rapid evaporation and increase in the void fraction. The pressure recovery that follows causes vapour condensation and stabilisation of the vapour amount on an appropriate level. So, most likely, it is rapid creation of the vapour that causes choking of the flow. Curves like those in Fig.12 \div Fig.14 can be obtained in the entire channel, attesting that we deal not only with evaporation but also with local condensation in time. Rapidly created vapour enters the part of the channel of constant cross-section area and causes stronger choking of the flow than in the case of pure water.

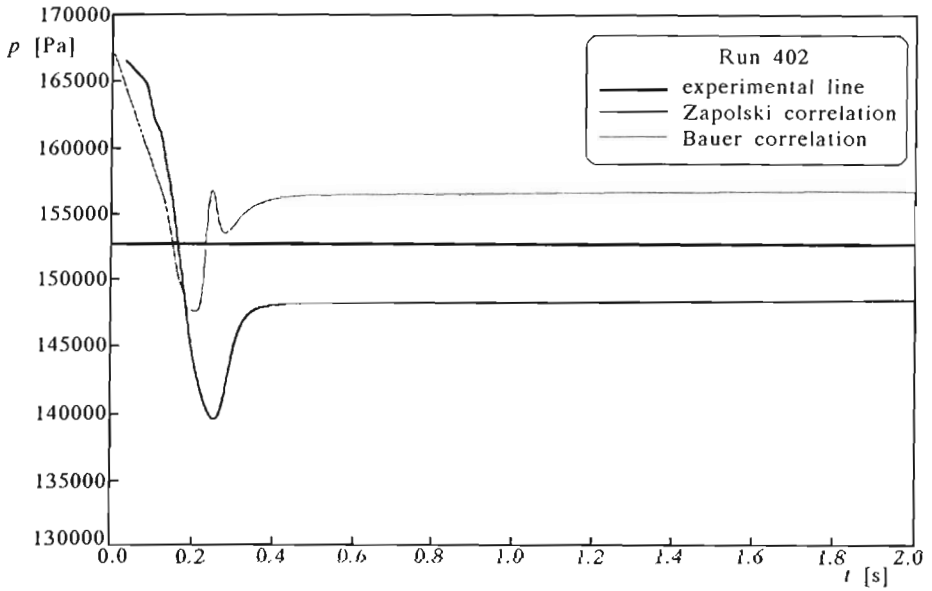


Fig. 12. Time-evolution of the pressure for run 402 calculated with the help of Zapolski's and Bauer's correlations

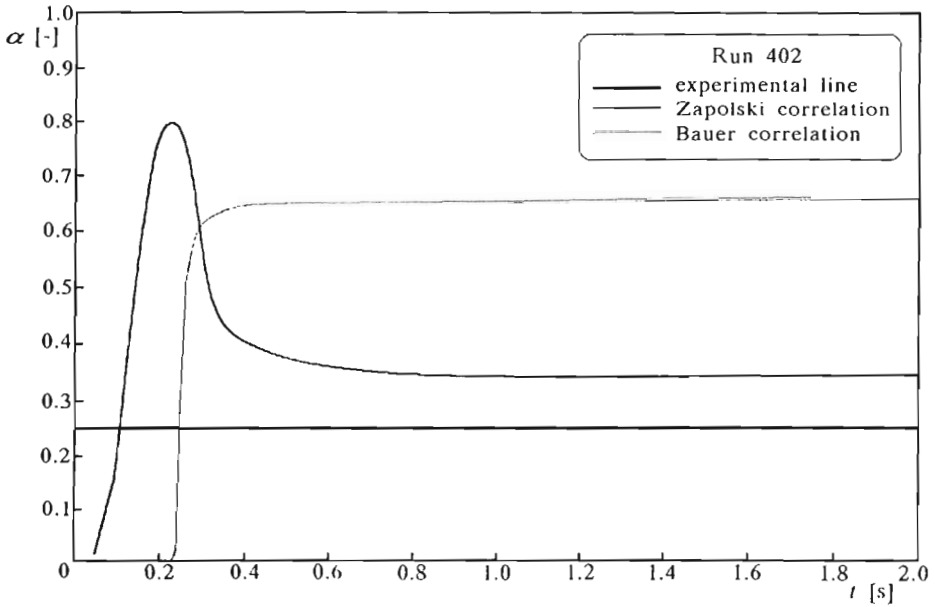


Fig. 13. Time-evolution of the void fraction for run 402 calculated with the help of Zapolski's and Bauer's correlations

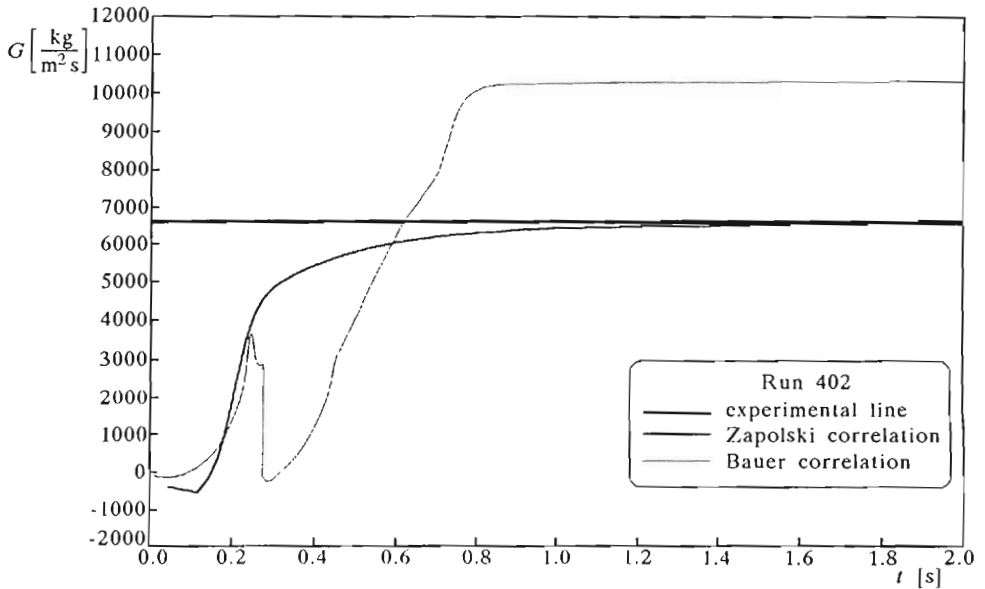


Fig. 14. Time-evolution of the mass flux for run 402 calculated with the help of Zapolski's and Bauer's correlations

For the sake of comparison, the profiles calculated with the help of Bauer's correlation are also shown. It is clearly seen that this correlation leads to a qualitatively different picture of the vapour production. The time-evolution of the void fraction does not have an extremum and there is no rapid evaporation and later condensation so characteristic for Zapolski's correlation. This is a result of taking into account the flow velocity in negative power which considerably increases the relaxation time at the initial stage of the flow when the flow velocities are still low. The minimum pressure is reached after some 0.2s and until this instant the flow velocity is lower than 1 m/s.

This fact is proved by another numerical experiment performed for the same channel, in which identical pressure differences between the inlet and the outlet were assumed and the inlet pressure was changed, keeping the temperature constant. As a result, the vapour-pressure line was reached at different parts of the channel and the location of the flash point was displaced. The same friction factor and correlation for the relaxation time were used in all runs. The results of this numerical experiment are collected in Table 2 and shown in Fig.15 and Fig.16.

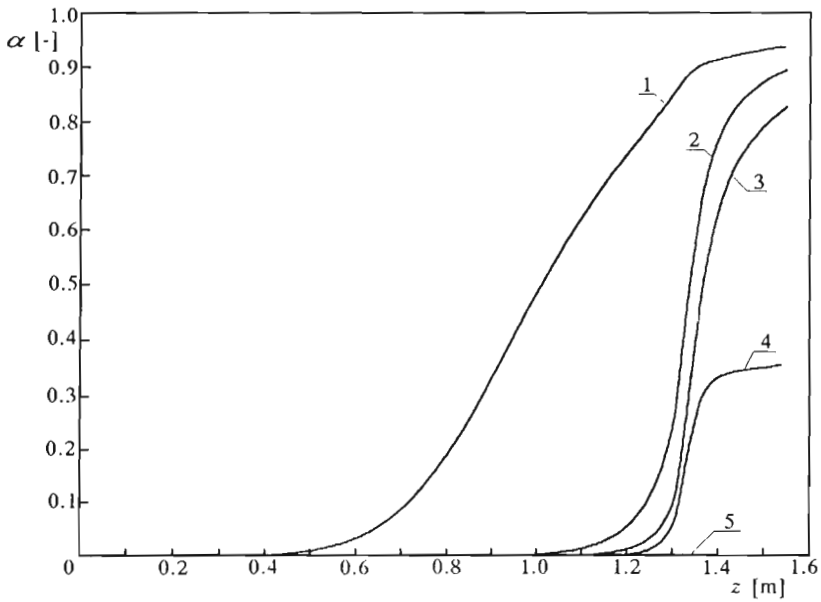


Fig. 15. Void fraction profiles calculated for different locations of the flash point; values of the parameter G_{in} for respective curves are given in Table 2

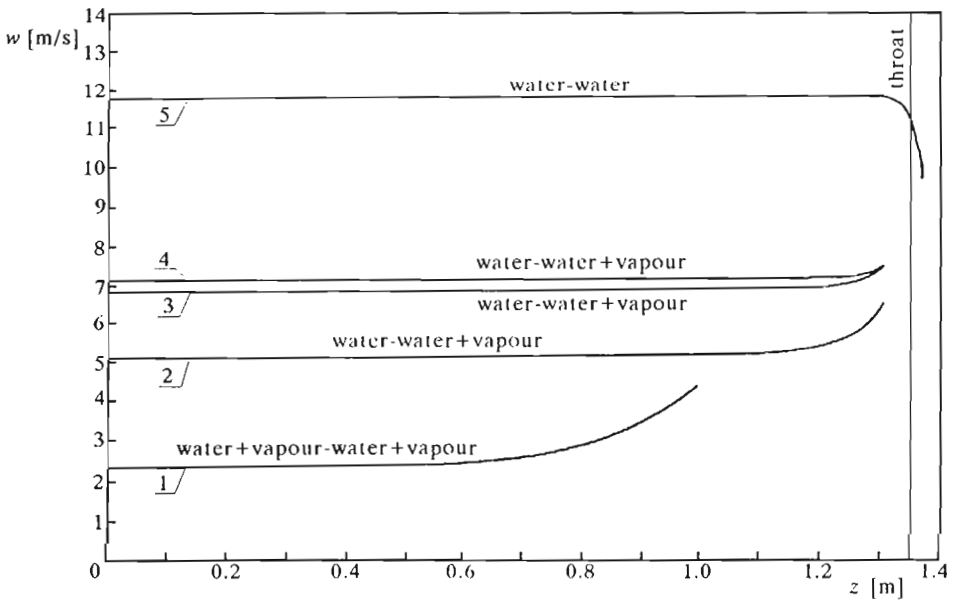


Fig. 16. Velocity profiles calculated for different locations of the flash point; values of the parameter P_{in} for respective curves are given in Table 2

Table 2

No.	P_{in} [bar]	P_{out} [bar]	ΔP [bar]	T [°C]	G_{in} [kg/m ² s]
1	1.740	1.268	0.472	116	2208
2	1.831	1.359	0.472	116	4800
3	1.928	1.456	0.472	116	6466
4	2.170	1.698	0.472	116	6741
5	3.552	3.080	0.472	116	11114

It is seen that the flow velocity at the inlet clearly depends on the location of the flash point. The more upstream the vapour appears in the channel, the lower is the flow velocity at the inlet, assuming still the same pressure difference. So, the possible reason of increased flow choking is overintensive generation of the vapour and its slow condensation downstream. Therefore, in order to achieve a higher flow velocity at the inlet, the friction factor should be decreased.

It is certain that the relaxation equation is entirely responsible for the production of the vapour in our model. But this equation employs an empirical correlation selected for steady flows. The flow velocity is not included in Zapolski's correlation and for low velocities it results in low values of the relaxation time and overproduction of the vapour. Finally, we obtain good results for the pressure and void fraction provided that the flow velocity is controlled by the friction factor. Our considerations are confirmed also by calculations performed with the help of Bauer's correlation which accounts for the flow velocity (see Fig.13 and Fig.14). As a result of using Bauer's correlation, we obtain large values of the relaxation time at low velocities and condensation is not observed. However, this correlation is far from perfect since in the steady state it underestimates the amount of the produced vapour.

7. Conclusions

Our calculations have proved that the nonequilibrium relaxation model describes well critical flows of two-phase liquid-vapour mixtures. Experimentally proved thermodynamic nonequilibrium which manifests itself by a metastable state of the liquid considerably influences the process of vapour generation. The production of the vapour is modelled by means of the relaxation-type evolution equation. Although the equation is very simple in its form and describes only one of the possible mechanisms of mass exchange, it represents well a complicated process of creation of the new phase. Nevertheless, an

exact value of the relaxation time is required to achieve good agreement with the experiment. The relaxation time is a characteristic time for the process of mass exchange and it conditions the intensity of this process in our model.

The *homogeneous relaxation model* turns out to be very sensitive to the local value of the relaxation time which may change from 1s to 0.01s. The correlations for the relaxation time worked out for steady flows fail when applied to non-steady calculations. An agreement with the experiment hinges then not only on the relaxation time but also on the friction factor, which is a free parameter of the model. Choosing an appropriate correlation for the relaxation time and finding numerically a suitable friction factor yield not only qualitative but even good quantitative agreement of the calculations with the experiment. Such agreement has been obtained during calculations made for several runs of the Moby Dick experiment, which is a classical measurement of the critical liquid-vapour flows.

To sum up, the nonequilibrium relaxation model supplemented with correct constitutive equations and empirical factors describes well two-phase flows in pipes and nozzles.

Acknowledgements

The authors wish to acknowledge the financial support received from the EEC under Grant ERB EV5VCT930289.

References

1. BAUER E.G., HOUDAYER G.R., SUREAU H.M., 1976, A Non Equilibrium Axial Flow Model and Application to Loss-of-Coolant Accident Analysis: the CLYSTERE System Code, Transient Two-Phase Flow, *Proceedings of the CSNI, Specialists Meeting* (Toronto, August 3-4, 1976), **1**, 429-458
2. BILICKI Z., KESTIN J., 1990, Physical Aspects of the Relaxation Model in Two-Phase Flow, *Proc. R. Soc. London*, **A428**, 379-397
3. BILICKI Z., KESTIN J., PRATT M.M., 1990, A Reinterpretation of the Results of the Moby Dick Experiments in Terms of the Nonequilibrium Model, *ASME Journal of Fluids Engineering*, **112**, 212-217
4. CHEN N.H., 1979, An Explicit Equation for Friction Factor in Pipes, *Ind. Eng. Chem. Fund.*, **18**, 296
5. DOWNAR-ZAPOLSKI P., BILICKI Z., BOLLE L., FRANCO J., 1996, The Nonequilibrium Relaxation Model for One-Dimensional Flashing Liquid Flow, *Int. J. Multiphase Flow*, **22**, 473-483
6. GOVIER G.W., AZIZ K., 1972, The Flow of Complex Mixtures in Pipes, Van Nostrand Reynhold Company, New York, 152-166

7. KARDAŚ D., 1994, Analiza wpływu członów dyssypacyjnych na numeryczne rozwiązanie niestacjonarnych przepływów dwufazowych, Praca doktorska, IMP PAN
8. KARDAŚ D., BILICKI Z., 1994, Zbiór funkcji termodynamicznych dla obszaru metastabilnego wody i pary. Opracowanie wewnętrzne IMP PAN, No.371/94, 1-136, Gdańsk
9. MANDELSTAM L.I., LEONTOVICH E.M., 1937, A Theory of Sound Absorption in Liquids, *J. Exp. Theor. Physics*, 7, 438-449
10. REOCREUX M., 1974, Contribution a l'étude des debits critiques en écoulement diphasique eau-vapeur, Ph.D. Thesis, Université Scientifique et Medicale de Grenoble
11. RICHARDSON B.L., 1958, Some Problems in Horizontal Two-Phase Two-Component Flow, *ANL-5949*
12. SAHA P., JO J.H., NEYMOTIN L., ROHATGI U.S., SLOVIK G., 1982, Independent Assessment of TRAC-PD2 and RELAP5/MOD1 Codes at BNL in FY 1981, *BNL-NUREG-51645*, December

Numeryczne obliczenia eksperymentu Moby Dick z użyciem nierównowagowego modelu relaksacyjnego

Streszczenie

W pracy przedstawiono numeryczne obliczenia eksperymentu Moby Dick z użyciem nierównowagowego modelu relaksacyjnego. Do obliczeń użyto programu rozwiązującego zagadnienie przepływu niestacjonarnego. Zbadano wpływ zastosowanych korelacji na czas relaksacji na przebieg produkcji pary oraz przedyskutowano problem doboru współczynnika tarcia dla przepływów dwufazowych. Wyniki obliczeń numerycznych porównano z przebiegami doświadczalnymi i na tej podstawie oceniono przydatność omawianego modelu do opisu krytycznych przepływów wody i pary.

Manuscript received October 30, 1996; accepted for print November 29, 1996